Approximate Stress Intensity Factors and Notch Stresses for Common Spot-Welded Specimens

The formulas developed will be helpful for testing, design and optimization of fatigue-resistant spot welds

BY S. ZHANG

ABSTRACT. Stress intensity factors and notch stresses are approximated analytically for common spot-welded specimens. The stress intensity factors and notch stresses at spot welds in the specimens are directly related via a number of formulas to the applied loads and the weld and specimen geometries. Comparisons with some available finite element results from the literature show that the analytical approximations are acceptable for engineering applications. The formulas are, nevertheless, of limited value because they are still not systematically validated by finite element results with systematic variations of the weld and specimen geometries. As an example of application, the formulas are employed to correlate some fatigue test data gathered from different weld geometries and different specimen configurations with the scatter-band of the data being substantially reduced.

Introduction

The fatigue test data of spot welds in the form of load vs. life to failure gathered from different weld geometries or specimen configurations scatter to such extent that only with severe restrictions is it possible to reasonably compare the fatigue strength or transfer it among different weld geometries or specimen configurations. Accordingly, appropriate correlating parameters are sought to overcome this problem. Pook (Ref. 1) and Yuuki, *et al.* (Ref. 2), have shown that the test data are much less scattered if making use of the stress intensity factor as a correlating parameter. Similarly, notch stress is another candidate correlating parameter (Refs. 3, 4). However, determining stress intensity factors and notch stresses at spot welds can be a costly process — even for simple tensile-shear or cross-tension specimens. It often demands refined three-dimensional finite element analysis, with extraction of stress intensities from the stresses and displacements in the vicinity of the spot welds. Obviously, a simple procedure for predicting the stress intensity factors and notch stresses with acceptable accuracy for common spot-welded specimens is desired in practice.

Stress intensity factors, *J*-integral and notch stresses at spot welds in the tensile-shear, cross-tension and coach-peel specimens were approximated analytically (Ref. 4) ending up with a number of simple formulas where the stress intensity factors, *J*-integral and notch stresses were directly related to the applied loads and to the weld and specimen geometries. The approximations were found to be acceptable for engineering applications, in comparison to finite element results. The same procedure is applied here to some component-like spot-welded specimens, *i.e.*, the hat profile specimens, the H-shaped specimens (Refs. 5, 6) and the double-cup specimen (Ref. 7). The stress intensity factors and notch stresses for these specimens are derived from simple formulas (Ref. 4), in some cases with the aid of superposition. The *J*-integral is not considered because superposition is not valid for it.

Simple Specimens

The formulas of stress intensity factors and notch stresses for the simple specimens under tensile-shear, cross-tension and coach-peel loads are the basis of obtaining similar formulas for the more complicated component-like specimens. The stress intensity factors K_I, K_{II} and K_{III}, notch stress σ_k and circumferential shear notch stress τ_k for the tensile-shear specimen (Fig. 1) are quoted here (Ref. 4) with tensile-shear force F, sheet thickness t, nugget diameter d and notch-root radius ρ at the nugget edge

$$K_I = \frac{\sqrt{3}F}{2\pi d\sqrt{t}}, \tag{1}$$

$$K_{II} = \frac{2F}{\pi d\sqrt{t}}, \tag{2}$$

$$K_{III} = \frac{\sqrt{2}F}{\pi d\sqrt{t}}, \tag{3}$$

$$\sigma_k = \frac{4F}{\pi dt}\left(1+\frac{\sqrt{3}+\sqrt{19}}{8\sqrt{\pi}}\sqrt{\frac{t}{\rho}}\right), \tag{4}$$

$$\tau_k = \frac{F}{\pi dt}\left(1+\sqrt{\frac{2}{\pi}}\sqrt{\frac{t}{\rho}}\right). \tag{5}$$

Similarly, the formulas are listed as follows for the cross-tension specimen (Fig. 2) with spacing c of cross-tension force T (Ref. 4):

$$K_I = \frac{3\sqrt{3}cT}{16\pi dt\sqrt{t}}, \tag{6}$$

$$K_{II} = \frac{3cT}{32\pi dt\sqrt{t}}, \tag{7}$$

$$\sigma_k = \frac{3cT}{4\pi dt^2}\left(1+\frac{2\sqrt{3}+\sqrt{13}}{8\sqrt{\pi}}\sqrt{\frac{t}{\rho}}\right). \tag{8}$$

The formulas for the coach-peel specimen (Fig. 3) read with eccentricity e of coach-peel force P (Ref. 4):

$$K_I = \frac{2\sqrt{3}eP}{\pi dt\sqrt{t}}, \tag{9}$$

KEY WORDS

Stress Intensity Factor
Notch Stress
Spot-Welded Specimen
Fracture
Fatigue

S. ZHANG is with Research and Technology, DaimlerChrysler AG, Stuttgart, Germany.

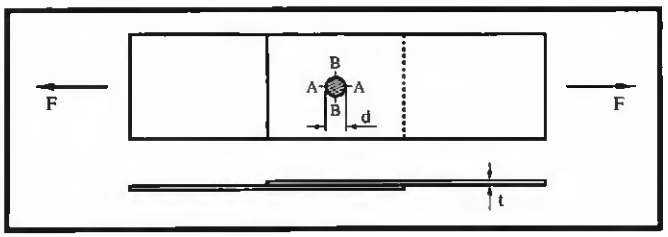


Fig. 1 — Tensile-shear specimen.

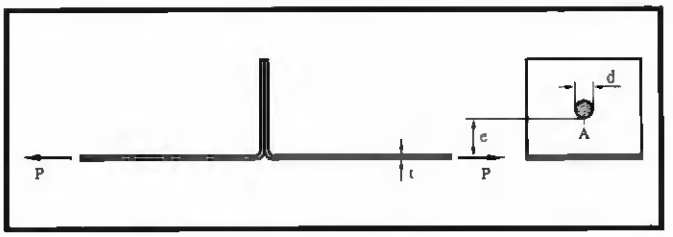


Fig. 3 — Coach-peel specimen.

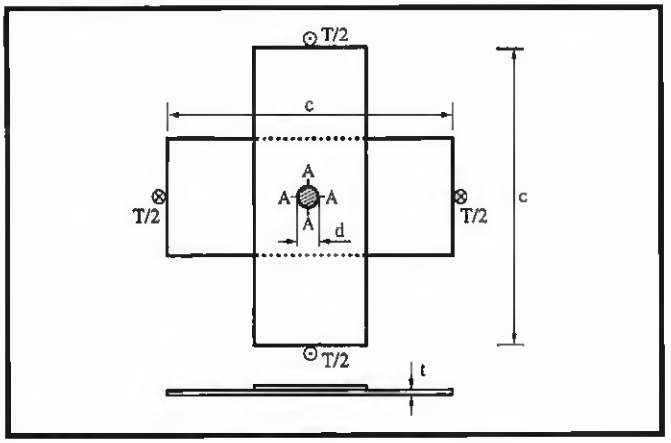


Fig. 2 — Cross-tension specimen.

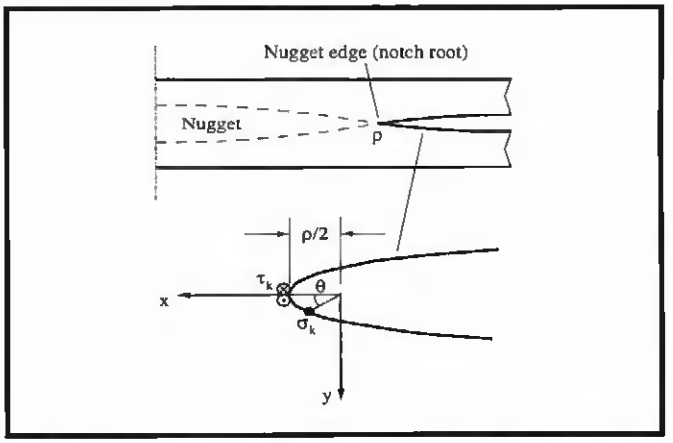


Fig. 4 — Notch of root radius ρ and notch stresses on the nugget edge.

$$\sigma_k = \frac{6eP}{\pi dt^2}\left(1+\frac{2}{\sqrt{3\pi}}\sqrt{\frac{t}{\rho}}\right). \qquad (10)$$

The above formulas actually express the maxima of the stress intensity factors and notch stresses on the nugget edge. The stress intensity factors K_I and K_{II}, and notch stress σ_k occur at the leading vertex of the spot weld in line with the applied force (point A in Figs. 1–3), whereas K_{III} and τ_k occur at the side vertex (point B in Fig. 1). The stress intensity factor K_{III} and the circumferential shear notch stress τ_k for the cross-tension specimen and K_{II}, K_{III} and τ_k for the coach-peel specimen vanish due to symmetry conditions.

The following relations between stress intensity factors and notch stresses, which are slightly reformulated (Ref. 4), are also needed; subsequently

$$\sigma_k = \sigma_n + \frac{K_I \pm \sqrt{K_I^2 + K_{II}^2}}{\sqrt{\pi\rho}}, \qquad (11)$$

$$\tau_k = \tau_n + \frac{K_{III}}{\sqrt{\pi\rho}}, \qquad (12)$$

where σ_n and τ_n are nominal structural stresses at spot welds. The square root in Equation 11 takes the plus sign when $K_I \geq 0$ and the minus sign when $K_I < 0$. The notch-root radius, designated as ρ throughout this paper, is defined in the radial cross sections of a spot-welded joint as shown in Fig. 4. The notch stress σ_k occurs at an angle of $\theta = -\arctan(K_{II}/K_I)$ and τ_k at $\theta = 0$ from the extension plane of the crack. Equations 11 and 12 were derived by locating the maximum tangential stress along the interior surface of the notch root. This was done by differentiating the tangential stress, which had been expressed by K_I and K_{II} (Ref. 3), with respect to θ and setting the derivative equal to zero.

Hat Profile Specimens

Finite element (Ref. 8) and experimental (Ref. 9) results have shown that there is no major difference between single- and double-hat profile specimens in terms of stress intensities at the spot welds, as long as the enclosed cross-sectional area of the specimens is the same. Consequently, the two specimen configurations are not distinguished here from each other, unless there is a specific reason to do so. For the hat profile specimens under torsion, as shown in Fig. 5, the local loading condition at spot welds in the specimens is predominantly pure shear, and the shear force is related to the torsional moment M_t, spot pitch a and enclosed cross-sectional area A (Refs. 8–10):

$$F = \frac{aM_t}{2A}. \qquad (13)$$

The stress intensities at the spot welds caused by the shear force are similar to those in the case of the tensile-shear specimen. The main difference between the two cases is that $K_I \approx 0$ for the hat profile specimens. A correction factor k (Ref. 9) should be introduced for the stress intensities K_{II} and σ_k at the leading vertex of the spot weld (point A in Fig. 5) in line with the principal loading direction, to account for the relation between the mean shear stress in the spot weld and the maximum radial stress at the nugget edge. Two slightly different values were given (Ref. 9) for the single- and double-hat profile specimens. An average value of $k = 1.23$ from the two values is introduced here, for both single- and double-hat profile specimens. The correction is not necessary for the circumferential shear stress intensities K_{III} and τ_k, at the side vertex (point B in Fig. 5), because K_{III} and τ_k are not related to the radial stress. The stress intensity factors for the hat profile specimens are then obtained by substituting Equation 13 into Equations 2 and 3

$$K_{II} = \frac{kaM_t}{\pi Ad\sqrt{t}}, \qquad (14)$$

$$K_{III} = \frac{aM_t}{\sqrt{2}\pi Ad\sqrt{t}}. \qquad (15)$$

The nominal structural stresses at spot welds in the hat profile specimens are approximated as follows (Ref. 11):

$$\sigma_n = \frac{2aM_t}{\pi dtA}, \tag{16}$$

$$\tau_n = \frac{aM_t}{2\pi dtA}. \tag{17}$$

The notch stresses are then derived from Equations 11 and 12 with the knowledge of Equations 14 through 17

$$\sigma_k = \frac{2aM_t}{\pi dtA}\left(1 + \frac{k}{2\sqrt{\pi}}\sqrt{\frac{t}{\rho}}\right), \tag{18}$$

$$\tau_k = \frac{aM_t}{2\pi dtA}\left(1 + \sqrt{\frac{2}{\pi}}\sqrt{\frac{t}{\rho}}\right). \tag{19}$$

The stress intensity factors predicted by Equations 14 and 15 are compared in Table 1 with the finite element results from Ref. 8. No comparison is made for the notch stresses because no finite element results are available. It is noted that the points A and B marked in Fig. 5 are the theoretical positions of the maximum stress intensities. In reality, the maximum stress intensities may shift slightly from their theoretical positions, especially for the single-hat profile specimen.

H-Shaped Specimens

Spot-welded specimens with an H-shaped cross section as shown in Figs. 6 and 7 were proposed by Singh (Refs. 5, 6) for fatigue testing of spot welds. The spot welds in the specimen as shown in Fig. 6 are mainly under tensile shear, whereas those as shown in Fig. 7 are mainly under coach peel. Therefore, the stress intensity factors and notch stresses for the H-shaped specimens can be approximated by the results from the tensile-shear and coach-peel specimens. Similar to the hat profile specimens, a correction factor k for the stress intensities in principal loading direction (point A in Figs. 6 and 7) should be introduced. The principal loading direction coincides with the row of spot welds along the flange for the hat profile specimens, whereas it is perpendicular to the row of spot welds in the case of the H-shaped specimens. Therefore, $k = 1.12$ is introduced here for the H-shaped specimens, which is not identical to the k value for the hat profile specimens. For the H-shaped specimen under total tensile-shear force F (Fig. 6) with the total number N of spot welds, the stress intensity factors and notch stresses are obtained as follows:

$$K_I = \frac{\sqrt{3}kF}{2\pi Nd\sqrt{t}}, \tag{20}$$

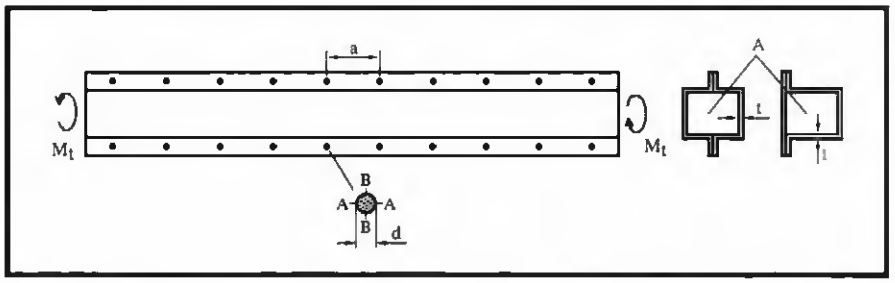


Fig. 5 — Hat profile specimens.

$$K_{II} = \frac{2kF}{\pi Nd\sqrt{t}}, \tag{21}$$

$$K_{III} = \frac{\sqrt{2}F}{\pi Nd\sqrt{t}}, \tag{22}$$

$$\sigma_k = \frac{4kF}{\pi Ndt}\left(1 + \frac{\sqrt{3}+\sqrt{19}}{8\sqrt{\pi}}\sqrt{\frac{t}{\rho}}\right), \tag{23}$$

$$\tau_k = \frac{F}{\pi Ndt}\left(1 + \sqrt{\frac{2}{\pi}}\sqrt{\frac{t}{\rho}}\right). \tag{24}$$

The stress intensity factors predicted by Equations 20–22 are compared in Table 2 with the finite element results (Ref. 12).

For the H-shaped specimen under total coach-peel force P, the stress intensity factor and notch stress are with eccentricity e

$$K_I = \frac{2\sqrt{3}keP}{\pi Ndt\sqrt{t}}, \tag{25}$$

$$\sigma_k = \frac{6keP}{\pi Ndt^2}\left(1 + \frac{2}{\sqrt{3\pi}}\sqrt{\frac{t}{\rho}}\right). \tag{26}$$

The stress intensity factor predicted for

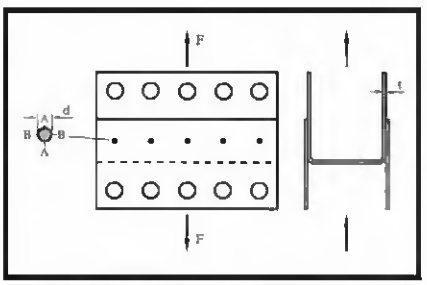


Fig. 6 — H-shaped specimen with spot welds under tensile shear.

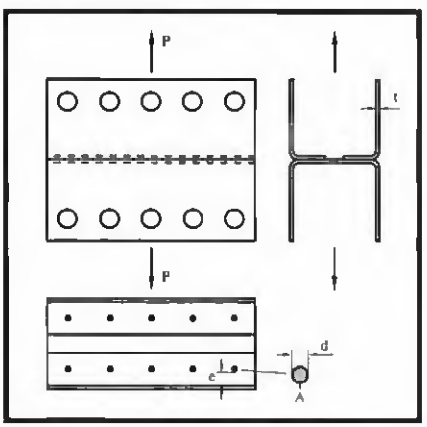


Fig. 7 — H-shaped specimen with spot welds under coach peel.

Table 1 — Stress Intensity Factors for Single- and Double-Hat Profile Specimens under Torsional Moment $M_t = 10^5$ Nmm with Sheet Thickness $t = 1$ mm, Nugget Diameter $d = 5$ mm, Spot Pitch $a = 50$ mm and Enclosed Cross-Sectional Area $A = 2500$ mm^2

Authors	K_{II} (N/mm$^{3/2}$)	K_{III} (N/mm$^{3/2}$)
Radaj (Ref. 8), single hat	154.2	93.0
Radaj (Ref. 8), double hat	152.0	91.6
Zhang, Equations 14, 15	156.6	90.0

Table 2 — Stress Intensity Factors for an H-Shaped Specimen with Ten Spot Welds under Total Tensile-Shear Force $F = 10$ kN with Sheet Thickness $t = 1$ mm and Nugget Diameter $d = 5$ mm

Authors	K_I (N/mm$^{3/2}$)	K_{II} (N/mm$^{3/2}$)	K_{III} (N/mm$^{3/2}$)
Radaj and Giering (Ref. 12)	74.1	143.0	63.6
Zhang, Equations 20–22	61.7	142.6	90.0

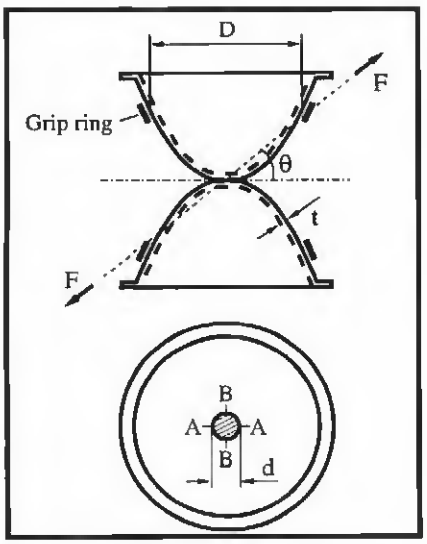


Fig. 8 — Double-cup specimen.

an H-shaped specimen with ten spot welds under the total coach-peel force $P = 1$ kN with sheet thickness $t = 1$ mm, nugget diameter $d = 5$ mm and eccentricity $e = 7$ mm is $K_I = 172.9$ N/mm$^{3/2}$. The corresponding finite element result is $K_I = 176.0$ N/mm$^{3/2}$ (Ref. 12). The notch stresses are not compared for the two H-shaped specimens due to a lack of corresponding finite element results. It is assumed that the loading condition at all spot welds in the H-shaped specimens is approximately the same. In reality, the stress intensities at the spot welds near the two ends of the specimens may show some difference from those in the middle.

Double-Cup Specimen

A double-cup specimen (DC-specimen, Fig. 8) was recently proposed by Gieske, *et al.* (Ref. 7), for the static and fatigue testing of spot welds. The loading condition at the spot weld can be investigated with the same specimen by changing the loading direction (in practice by changing the position of the specimen on the test machine). The tensile shear and cross tension are the two extreme loading cases for the specimen. The formulas for the tensile-shear and cross-tension specimens are employed here to construct the stress intensity factors and notch stress for the DC specimen based on superposition. The tensile-shear and cross-tension forces are the two projections $F\cos\theta$ and $F\sin\theta$ of the total force F, which inclines at an angle θ to the cross-sectional plane of the spot weld as shown in Fig. 8. The following formulas are derived from introducing $F\cos\theta$ into Equations 1, 2 and 4 and $F\sin\theta$ into Equations 6 and 8, with an appropriate superposition of the contributions from the tensile-shear and cross-tension forces

$$K_I = \frac{\sqrt{3}F}{2\pi d\sqrt{t}}\left(\cos\theta + \frac{3D}{8t}\sin\theta\right), \qquad (27)$$

$$K_{II} = \frac{2F}{\pi d\sqrt{t}}\cos\theta, \qquad (28)$$

$$\sigma_k = \frac{4F}{\pi dt}\left\{\cos\theta + \frac{3D}{32t}\sin\theta + \frac{1}{8\sqrt{\pi}}\left[\left(\sqrt{3}+\sqrt{19}\right)\cos\theta + \frac{3\sqrt{3}D}{8t}\sin\theta\right]\sqrt{\frac{t}{\rho}}\right\}, \qquad (29)$$

where D is diameter of the grip ring through which the force F is applied to the specimen. The circumferential shear stress intensities K_{III} and τ_k vanish due to symmetry conditions. The stress intensity factors predicted by Equations 27 and 28 are compared in Table 3 with the finite element results (Ref. 13).

Application Example and Discussions

As an example of application, the formulas given in the previous sections are now utilized to correlate some fatigue test data from the literature for the tensile-shear (Ref. 14), cross-tension (Ref. 15), coach-peel (Ref. 15), hat profile (Ref. 9), H-shaped (Ref. 16) and double-cup (Ref. 17) specimens. The H-shaped specimen has two variants: with spot welds under tensile shear (ts) and with spot welds under coach peel (cp). For the double-cup specimen, there are five variants: $\theta = 0°$ (I); $\theta = 15°$ (II); $\theta = 30°$ (III); $\theta = 60°$ (IV) and $\theta = 90°$ (V). The weld and specimen geometries of these specimens are quite different, with sheet thicknesses ranging from 0.8 to 3.2 mm and nugget diameters from 4.1 to 10.0 mm. The materials and the stress ratio R also differ to some extent. Another difference lies in the failure definition used by various investigators. The failure was defined as crack initiation at spot welds, except for the H-shaped specimens whose failure was identified indirectly by a 40% loss of the initial stiffness of the specimens. The original test data were collected in the form of load range vs. life to failure. As expected, the test data in that form exhibit considerable scatter and some data — such as those from the hat profile specimen — are not even comparable because the applied load is a torsional moment for the hat profile specimen, whereas it is force for the rest. The test data, in terms of load range, are converted with the aid of the formulas in the previous sections into the form of equiv-

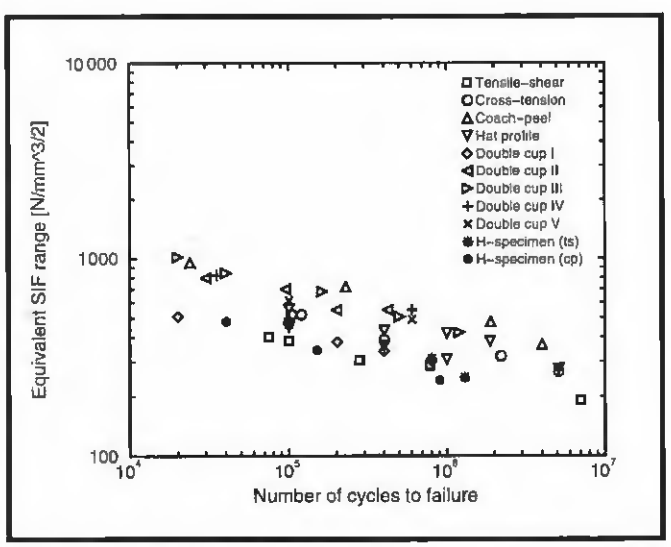


Fig. 9 — Equivalent stress intensity factor range vs. life to failure for various specimens with different weld and specimen geometries.

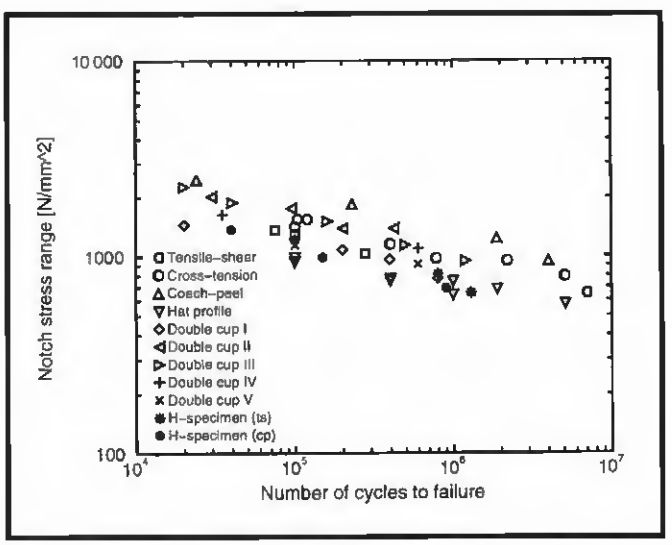


Fig. 10 — Notch stress range vs. life to failure for various specimens with different weld and specimen geometries.

alent stress intensity factor range vs. life to failure (Fig. 9) and notch stress range vs. life to failure — Fig. 10. The equivalent stress intensity factor is defined as follows (Ref. 4):

$$K_{eq} = \pm\sqrt{K_I^2 + \alpha K_{II}^2 + \beta K_{III}^2}, \qquad (30)$$

where the square root takes the plus sign when $K_I \geq 0$ and the minus sign when $K_I < 0$. This is a K_I-equivalent definition. The sign of the equivalent stress intensity factor accounts for the opening (+) and closure (–) of a crack. The two parameters, α and β, are weight factors of the mode II and mode III stress intensities, whose values are normally not far from 1.0. In this example, $\alpha = \beta = 1.0$ is introduced. In the calculation of notch stress, the notch-root radius ρ =1.0 mm is assumed for all specimens, according to Radaj (Ref. 8). It is noted that the stress intensity factors K_I and K_{II} and the notch stress σ_k take the maxima at the leading vertex of the spot weld (point A in Figs. 1–3 and 5–8) and the minima (theoretically zero) at the side vertex (point B in the figures), whereas K_{III} and τ_k are just opposite. Since the circumferential shear stress intensities K_{III} and τ_k are normally smaller than K_I or K_{II} and σ_k, only the equivalent stress intensity factor based on K_I and K_{II} and the notch stress σ_k are relevant in correlating the test data. It can be seen from Figs. 9 and 10 that the test data — in terms of both stress intensity factor and notch stress — have fallen into a relatively narrow band. This indicates that the formulas can be used to correlate fatigue test data across different specimen configurations and across different weld and specimen geometries. The results of the tensile-shear specimen, DC-specimen under tensile shear and H-shaped specimen under coach peel are considerably lower than the rest (Fig. 9), whereas the situation is improved in Fig. 10. It appears that the correlation based on notch stress is, to some extent, better than that based on stress intensity factors. This would mean that the fatigue strength of spot welds, to some extent, could be better predicted in terms of notch stress. This may be explained by the fact that a spot-welded joint looks more like a blunt crack where notch stress is of relevance, than like a sharp crack where stress intensity factors are of relevance.

When fatigue test data for spot welds are transferable among different specimens based on stress intensity factor or notch stress, the next question is how to transfer the test data from specimens to components or structures for fatigue predictions. In this case, the main issue is the calculation of stress intensity factors or notch stresses at spot welds in the components or structures. The stress intensity factors and notch stresses at a spot weld in components or structures (Ref. 18) can be calculated with the knowledge of the structural stresses σ_{ui}, σ_{uo}, σ_{li}, σ_{lo}, τ_{ui}, τ_{li}, τ_{qu} and τ_{ql} around the spot weld (Fig. 11):

$$K_I = \frac{1}{6}\left[\frac{\sqrt{3}}{2}(\sigma_{ui} - \sigma_{uo} + \sigma_{li} - \sigma_{lo}) + 5\sqrt{2}(\tau_{qu} - \tau_{ql})\right]\sqrt{t}, \qquad (31)$$

$$K_{II} = \left[\frac{1}{4}(\sigma_{ui} - \sigma_{li}) + \frac{2}{3\sqrt{5}}(\tau_{qu} + \tau_{ql})\right]\sqrt{t}, \qquad (32)$$

$$K_{III} = \frac{\sqrt{2}}{2}(\tau_{ui} - \tau_{li})\sqrt{t}, \qquad (33)$$

Table 3 — Stress Intensity Factors K_I and K_{II} (N/mm$^{3/2}$) in the Two Extreme Cases of Tensile-Shear ($\theta = 0$) and Cross-Tension ($\theta = \pi/2$) for DC-Specimen with Sheet Thickness $t = 1$ mm, Nugget Diameter $d = 5$ mm and Grip Ring Diameter $D = 43.7$ mm

Authors	K_I ($F = 0.1$ kN, $\theta = \pi/2$)	K_{II} ($F = 1$ kN, $\theta = 0$)
Radaj and Giering (Ref. 13)	82.0	132.0
Zhang, Equations 27, 28	90.3	127.3

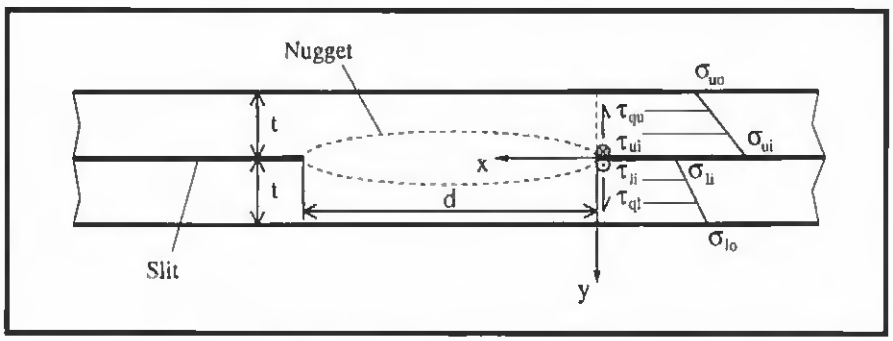


Fig. 11 — Structural stresses around a spot weld.

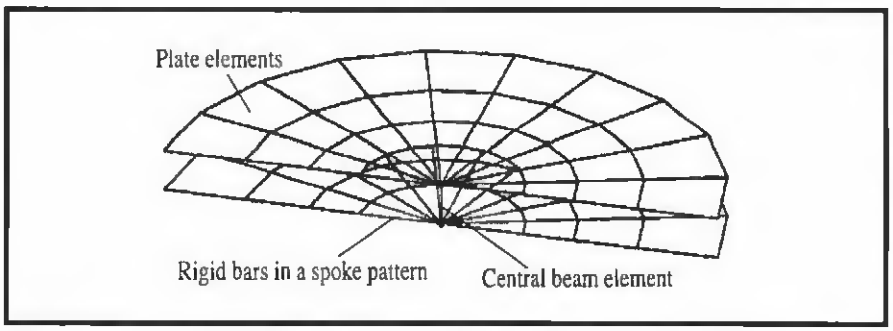


Fig. 12 — Finite element model for spot welds: a central beam element with diameter of nugget diameter d *coupled through rigid bars in a spoke pattern (also with diameter of* d*) with plate elements.*

$$\sigma_k = \sigma_n + \frac{1}{4\sqrt{3}\pi}\sqrt{\frac{t}{\rho}}\left\{\sigma_{ui} - \sigma_{uo} + \sigma_{li} - \sigma_{lo} \pm \left[2(\sigma_{ui} - \sigma_{li})^2 + (\sigma_{uo} - \sigma_{lo})^2 + 2\left(\sigma_{ui}^2 + \sigma_{li}^2 - \sigma_{ui}\sigma_{uo} - \sigma_{ui}\sigma_{lo} - \sigma_{uo}\sigma_{lo} - \sigma_{li}\sigma_{lo}\right)\right]^{1/2}\right\}, \qquad (34)$$

$$\tau_k = \tau_n + \frac{1}{\sqrt{2\pi}}(\tau_{ui} - \tau_{li})\sqrt{\frac{t}{\rho}}, \qquad (35)$$

where σ_n and τ_n are nominal stresses at spot welds. The combined sign "±" in Equation 34 takes the plus if $\sigma_{ui} - \sigma_{uo} + \sigma_{li} - \sigma_{lo} \geq 0$ and the minus if $\sigma_{ui} - \sigma_{uo} + \sigma_{li} - \sigma_{lo} < 0$. The above equations are valid for spot welds between sheets of the same material and equal thickness. For spot welds between sheets of dissimilar materials and unequal thickness, a general solution is given in Ref. 19 for stress intensity factors. The structural stresses in

Equations 31–35 normally vary from edge point to edge point along the periphery of the nugget. Therefore, it is necessary to calculate the stress intensity factors and notch stresses in all directions around the spot weld to find the maxima of the stress intensities. In the calculation of the structural stresses, the stress singularity at the nugget edge should be suppressed by appropriate finite element modeling (Ref. 8). A very fine mesh is often required for a reliable prediction of the structural stresses. If this becomes impractical for a structure with many spot welds, the stress intensity factors and notch stresses can be estimated based on the interface forces F_x, F_y and F_z and moments M_x, M_y and M_z that a spot weld transfers from one sheet to another (Refs. 4, 18):

$$K_I = \frac{\sqrt{3}F}{2\pi d\sqrt{t}} + \frac{2\sqrt{3}M}{\pi dt\sqrt{t}} + \frac{5\sqrt{2}F_z}{3\pi d\sqrt{t}}, \quad (36)$$

$$K_{II} = \frac{2F}{\pi d\sqrt{t}}, \quad (37)$$

$$K_{III} = \frac{\sqrt{2}F}{\pi d\sqrt{t}} + \frac{2\sqrt{2}M_z}{\pi d^2\sqrt{t}}, \quad (38)$$

$$\sigma_k = \frac{4F}{\pi dt}\left(1 + \frac{\sqrt{3}+\sqrt{19}}{8\sqrt{\pi}}\sqrt{\frac{t}{\rho}}\right) + \frac{6M}{\pi dt^2}\left(1 + \frac{2}{\sqrt{3\pi}}\sqrt{\frac{t}{\rho}}\right) + \frac{4F_z}{\pi d^2}\left(1 + \frac{5d}{3\sqrt{2\pi}t}\sqrt{\frac{t}{\rho}}\right), \quad (39)$$

$$\tau_k = \left(\frac{F}{\pi dt} + \frac{2M_z}{\pi d^2 t}\right)\left(1 + \sqrt{\frac{2}{\pi}}\sqrt{\frac{t}{\rho}}\right), \quad (40)$$

with $F = \sqrt{F_x^2 + F_y^2}$, $M = \sqrt{M_x^2 + M_y^2}$ in the interface (joint face) and F_z, M_z along or about the z-axis, which is perpendicular to the interface. The interface forces and moments are also termed *joint face forces and moments* or *cross-sectional forces and moments*. When spot welds are modeled by beam elements — as is often the case — the interface forces and moments are simply obtained from the output of the beam elements. The finite element model for spot welds consists of a beam element, which is coupled through rigid bars in a spoke pattern with plate elements (midplanes), as shown in Fig. 12. The diameter of the beam element and the spoke pattern is equal to the diameter of the spot weld. Various finite element models of spot welds are discussed in Ref. 20. Mesh refinements around the beam element are needed if using this model to obtain the structural stresses around the spot weld. The stress intensity factors and notch stresses given by Equations 36–40 are the maxima of the stress intensities at a spot weld with K_I, K_{II} and σ_k at the leading vertex of the spot weld, in line with the principal loading direction analogous to point A in Figs. 1–3 and 5–8; and K_{III} and τ_k at the side vertex analogous to point B in the figures.

The formulas given in this paper are analytic approximations of the stress intensities at spot welds. The equivalent stress intensity factor and notch stress can be regarded as fatigue design parameters. In an early publication, a similar fatigue design parameter — termed stress index K_i — was proposed by Swellam, *et al.* (Ref. 21). The stress index was also based on stress intensity factors that were then approximated by superimposing the solutions from stress intensity factor handbooks for some two-dimensional configurations, which have similarities to a spot-welded joint. The equivalent stress intensity factor was then empirically modified as K_i against fatigue test data because the fatigue test data were not well correlated by the approximated stress intensity factors. The main reason for this is that the dependency of the stress intensity factors on sheet thickness and nugget diameter was not correctly expressed. The sheet thickness did not even appear in the expressions for the stress intensity factors in Ref. 21; on the other hand, the effect of nugget diameter was exaggerated in the expressions. Both the present method and Swellam's method are based on stress intensity factors at spot welds, but the expressions for the stress intensity factors are different. The present expressions seem more reliable because they are based on much more detailed analytic solutions given in Refs. 4 and 19. Another difference between the two methods is that Swellam's method needs an empirical correction to his analytic approximations of the stress intensity factors to achieve acceptable correlations; whereas, with the present method, acceptable correlations have been achieved without correction to the analytic approximations of the stress intensity factors. If empirical corrections are additionally made against comprehensive fatigue test data and against systematic finite element results, the present method can be further improved and more generalized. This cannot be done here because the author has no sufficient test data. It would be interesting in future investigations to combine the present formulas for the stress intensify factors with Swellam's method.

Conclusions

The formulas for the common specimens derived in the previous sections are analytical approximations of the stress intensity factors and notch stresses at spot welds between sheets of identical material and identical thickness. The influence of the weld and specimen geometries on the stress intensities at the spot welds is clearly indicated in the formulas. The comparisons with the finite element results for the given geometries show that the approximations are acceptable for engineering applications. Nevertheless, the formulas are of limited value because they are still not systematically validated by finite element results with systematic variations of the weld and specimen geometries. It is assumed that the nearest edge of spot welds is at least two nugget diameters away from free or loaded sheet edges and that spot welds are at least four nugget diameters apart in the case of multi-spot-welded specimens. As indicated in the application example, the formulas are suitable for correlating fatigue test data across different weld and specimen geometries and across different specimen configurations. The formulas should be helpful for testing, design and optimization of fatigue-resistant spot welds.

References

1. Pook, L. P. 1975. Fracture mechanics analysis of the fatigue behavior of spot welds. *International Journal of Fracture* 11: 173–176.

2. Yuuki, R., Ohira, T., Nakatsukasa, H., and Yi, W. 1986. Fracture mechanics analysis of the fatigue strength of various spot welded joints. Symposium on *Resistance Welding and Related Processes*, Osaka.

3. Lawrence, F. V., Wang, P. C., and Corten, H. T. 1983. An empirical method for estimating the fatigue resistance of tensile-shear spot-welds. SAE Paper 830035.

4. Zhang, S. 1997. Stress intensities at spot welds. *International Journal of Fracture* 88: 167–185.

5. Singh, S., Schmid, G., and Geo, S. 1991. Leichtbau durch optimierte Fügetechnik. *Metallkonstruktionen und Leichtbau — Möglichkeiten und Grenzen*, DVM, Berlin, pp. 407–426.

6. Singh, S. 1992. Fatigue testing of jointed sheet material specimens. IIW-Doc. III-998-92.

7. Gieske, D., and Hahn, O. 1994. Neue Einelementprobe zum Prüfen von Punktschweißverbindungen unter kombinierten Belastungen, *Schweißen und Schneiden* 46: 9–12.

8. Radaj, D. 1990. *Design and Analysis of Fatigue Resistant Welded Structures*, Abington Publishing, Cambridge, England.

9. Mabuchi, A., Niisawa, J., and Tomioka, N. 1986. Fatigue life prediction of spot-welded box-section beams under repeated torsion. SAE Paper 860603.

10. Tomioka, N., Niisawa, J., and Mabuchi, A. 1986. On theoretical analysis of stress at welding flange of spot welded box section member under torsion. SAE Paper 860602.

11. Radaj, D., and Zhang, S. 1996. Anschauliche Grundlagen für Kräfte und Spannungen in punktgeschweißten Überlappverbindungen. *Konstruktion* 48: 65–71.

12. Radaj, D. and Giering, A. 1994. Spot-welded H-specimen — The local stress parameters. *Materialpruefung* 36: 275–281.

13. Radaj, D., and Giering, A. 1995. Spot-welded double-cup specimen — The local stress parameters. *Materialpruefung* 37: 10–13.

14. Abe, H., Kataoka, S., and Satoh, T. 1986. Empirical formula for fatigue strength of single-welded joint specimens under tensile-shear repeated load. SAE Paper 860606.

15. Mizui, M., Sekine, T., Tsuzimura, A., Takasshima, T., and Shimazaki, Y. 1988. An evaluation of fatigue strength for various kinds of spot-welded test specimens. SAE Paper 880375.

16. Grubisic, V., *et al.* 1994. Verbesserung der Bauteilfestigkeit durch höherfeste Feinblechwerkstoffe und optimierte Fügeverfahren. Fügen im Leichtbau, *DVM-Bericht* 120: 47–61.

17. Hahn, O., Kurzok, J. R., and Rohde, A. 1998. Die Übertragbarkeit von Kennwerten einer punktgeschweißten Einelementprobe auf Bauteile. *ATZ Automobiltechnische Zeitschrift* 100: 228–232.

18. Zhang, S. 1999. Recovery of notch stress and stress intensity factors in finite element modeling of spot welds. NAFEMS World Congress on *Effective Engineering Analysis*, Newport, R.I.

19. Zhang, S. 1998. Stress intensities derived from stresses around a spot weld. *International Journal of Fracture* (accepted for publication).

20. Sheppard, S. D. 1993. Estimation of fatigue propagation life in resistance spot welds. ASTM STP 1211, pp. 169–185.

21. Swellam, M. H., Banas, G., and Lawrence, F. V. 1994. A fatigue design parameter for spot welds. *Fatigue and Fracture of Engineering Materials and Structures* 17: 1197–1204.

Preparation of Manuscripts for Submission to the *Welding Journal* Research Supplement

All authors should address themselves to the following questions when writing papers for submission to the Welding Research Supplement:

- Why was the work done?
- What was done?
- What was found?
- What is the significance of your results?
- What are your most important conclusions?

With those questions in mind, most authors can logically organize their material along the following lines, using suitable headings and subheadings to divide the paper.

1) **Abstract.** A concise summary of the major elements of the presentation, not exceeding 200 words, to help the reader decide if the information is for him or her.

2) **Introduction.** A short statement giving relevant background, purpose and scope to help orient the reader. Do not duplicate the abstract.

3) **Experimental Procedure, Materials, Equipment.**

4) **Results, Discussion.** The facts or data obtained and their evaluation.

5) **Conclusion.** An evaluation and interpretation of your results. Most often, this is what the readers remember.

6) **Acknowledgment, References and Appendix.**

Keep in mind that proper use of terms, abbreviations and symbols are important considerations in processing a manuscript for publication. For welding terminology, the *Welding Journal* adheres to ANSI/AWS A3.0-94, *Standard Welding Terms and Definitions.*

Papers submitted for consideration in the Welding Research Supplement are required to undergo Peer Review before acceptance for publication. Submit an original and one copy (double-spaced, with 1-in. margins on 8 ½ x 11-in. or A4 paper) of the manuscript. Submit the abstract only on a computer disk. The preferred format is from any Macintosh® word processor on a 3.5-in. double- or high-density disk. Other acceptable formats include ASCII text, Windows™ or DOS. A manuscript submission form should accompany the manuscript.

Tables and figures should be separate from the manuscript copy and only high-quality figures will be published. Figures should be original line art or glossy photos. Special instructions are required if figures are submitted by electronic means. To receive complete instructions and the manuscript submission form, please contact the Peer Review Coordinator, Doreen Kubish, at (305) 443-9353, ext. 275; FAX 305-443-7404; or write to the American Welding Society, 550 NW LeJeune Rd., Miami, FL 33126.